Site-selective C(sp³)–H oxidation of alkyl substrates devoid of functional handles

Author(s):
Lu, Yiheng; Knezevic, Melina; Prescimone, Alessandro; Goldfuss, Bernd; Tiefenbacher, Konrad

Publication date:
2025-03-13

Permanent link:
https://doi.org/https://doi.org/10.3929/ethz-b-000728244

Originally published in:
Chem 11(3), https://doi.org/10.1016/j.chempr.2025.102442

Chem

Site-selective C(sp^3)–H oxidation of alkyl substrates devoid of functional handles

Graphical abstract

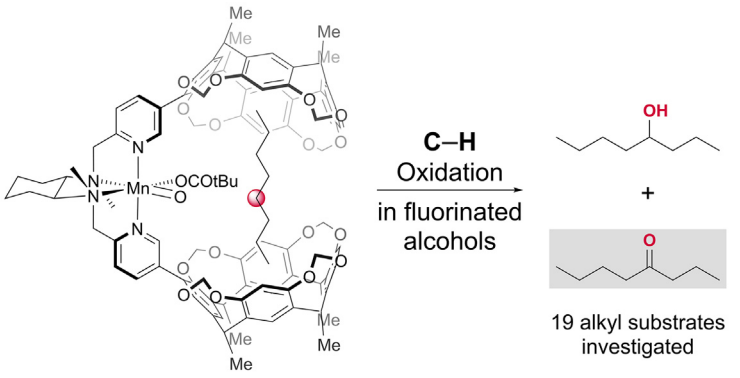

- Novel supramolecular C(sp^3)–H oxidation catalyst Mn(mcp)-RS_2
- No functional handle required for substrate binding
- Substrate binding driven by solvophobic effect
- Preferential oxidation of the fifth position on alkyl substrates

Highlights

- The solvophobic effect in fluorinated alcohols enables alkane-catalyst binding
- Substrate binding independent of a functional handle
- It facilitates the preferential oxidation of the fifth position on alkyl chains
- Such positions cannot be addressed with state-of-the-art oxidation catalysts

Authors

Yiheng Lu, Melina Knezevic, Alessandro Prescimone, Bernd Goldfuss, Konrad Tiefenbacher

Correspondence

konrad.tiefenbacher@unibas.ch

In brief

The site-selective C(sp^3)–H oxidation of non-activated hydrocarbons, which typically requires functional groups near the target site, remains challenging. This study introduces a supramolecular Mn(mcp)-RS_2 catalyst that harnesses the solvophobic effect in fluorinated alcohols to enable site-selective oxidation without functional-group dependence, achieving preferential oxidation at specific positions on aliphatic substrates.

Lu et al., 2025, Chem *11*, 102442
March 13, 2025
https://doi.org/10.1016/j.chempr.2025.102442

CellPress

Chem

CellPress
OPEN ACCESS

Article

Site-selective C(sp^3)–H oxidation of alkyl substrates devoid of functional handles

Yiheng Lu,[1] Melina Knezevic,[1] Alessandro Prescimone,[1] Bernd Goldfuss,[2] and Konrad Tiefenbacher[1,3,4,*]
[1]Department of Chemistry, University of Basel, Mattenstrasse 22, 4058 Basel, Switzerland
[2]Institute of Organic Chemistry, University of Cologne, Greinstrasse 4, 50939 Cologne, Germany
[3]Department of Biosystems Science and Engineering, ETH Zurich, Klingelbergstrasse 48, 4056 Basel, Switzerland
[4]Lead contact
*Correspondence: konrad.tiefenbacher@unibas.ch
https://doi.org/10.1016/j.chempr.2025.102442

THE BIGGER PICTURE The direct oxidation of hydrocarbons with suitable catalysts enables resource-efficient access to high-value functionalized molecules from inexpensive bulk starting materials. However, the site-selective oxidation of unactivated positions traditionally depends on functional groups that are already present on the substrate to enable substrate-catalyst binding. This article presents an alternative approach. Substrate-catalyst binding is enabled by the solvophobic effect in highly polar fluorinated alcohol solvents, enabling site-selective oxidations to the fifth position on the chain of alkane substrates. Such positions cannot be addressed with state-of-the-art oxidation catalysts. In the long term, this approach could enable the site-selective oxidation of complex carbon frameworks, facilitating the resource-efficient synthesis of drugs.

SUMMARY

Although the field of C(sp^3)–H oxidation has progressed tremendously over the last decades, the selective oxidation of non-activated positions on hydrocarbon skeletons is still highly challenging. It usually requires the presence of a suitable functional handle in proximity to the desired oxidation site. Here, we present a novel approach to catalyst-directed C–H oxidation that relies on substrate binding via the solvophobic effect in fluorinated alcohols and thus is independent of specific functional groups on the substrate. The supramolecular catalyst Mn(mcp)-RS_2 enables the preferential oxidation at the fifth position from the less-hindered side on aliphatic substrates.

INTRODUCTION

Aliphatic C–H oxidation represents a powerful transformation in organic synthesis in that it enables the direct functionalization of otherwise inert C–H bonds. However, functionalizing aliphatic C–H bonds is difficult because of the substantial bond strength for homolytic bond cleavage (bond-dissociation energy close to 100 kcal/mol),[1] as well as heterolytic cleavage ($pK_a \geq 50$).[2] Moreover, achieving selectivity is highly challenging because a multitude of C–H bonds with similar reactivity are present within the molecule. Chemists have developed highly innovative strategies for oxidizing some positions selectively. Importantly, the intrinsic reactivity of C–H bonds is now well understood and even predictable.[3–8] Electronic, steric, and stereoelectronic biases can be utilized for achieving the selective oxidation of a certain C–H bond in a given molecule. However, if an oxidation at a less reactive position is desired, the options are severely limited. If a functional handle at a precise distance to the desired oxidation position is available, directed intramolecular oxidations might be an option. Such approaches have been developed, for instance, by the Breslow,[9,10] Baran,[11] Hartwig,[12] and White[13] groups.

A very promising approach to selectively oxidizing a specific C–H bond is catalyst-directed C–H oxidation. It relies on attaching to the oxidation catalyst a binding motif that is able to orient the substrate in a specific manner toward the oxidant. This strategy, however, requires at least one appropriate functional group on the substrate to bind to the recognition motif linked to the catalyst.[14–20] Utilizing this strategy, the Di Stefano and Costas groups achieved the selective C8/C9 oxidation of aliphatic ammonium substrates by utilizing the crown-ether-modified Mn-/Fe(pdp) catalyst **1** (Figure 1A).[21,22] They assembled catalyst **1** by merging the well-established tetradentate iron and manganese aminopyridine complexes **2** and **3**, which have emerged as superior catalysts for the oxidation of non-activated C–H bonds,[5,23] with an ammonium-binding crown ether motif. This constituted a major achievement given that the selective oxidation of unactivated positions far away from functional handles

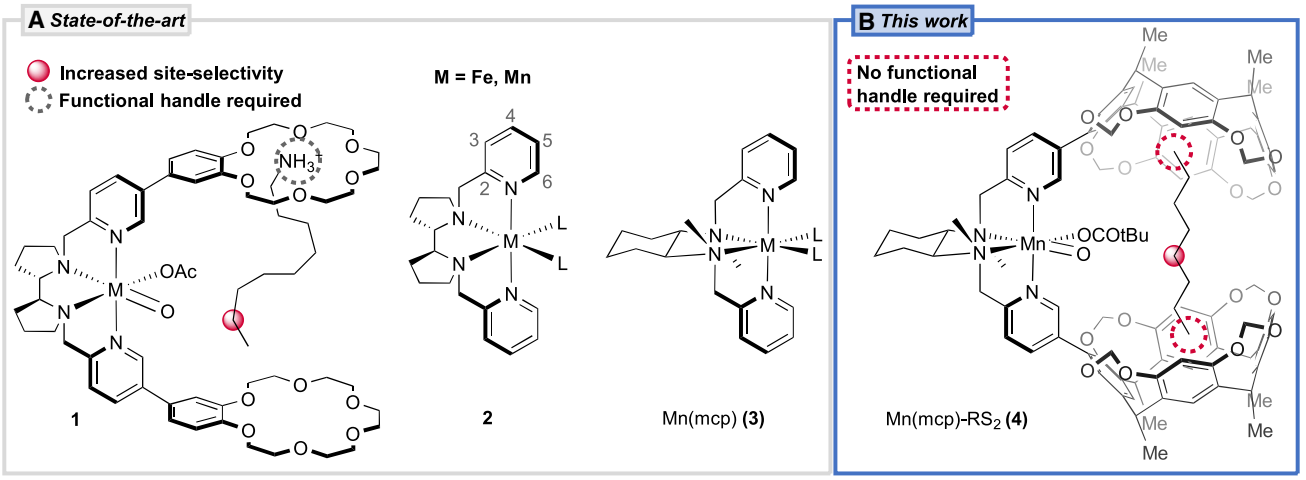

Figure 1. Nonheme C–H oxidation catalysts

(A) State-of-the-art nonheme C–H oxidation catalysts **1**–**3**.

(B) Supramolecular catalyst **4** is capable of oxidizing C(5)–H bonds on aliphatic substrates devoid of functional handles.

remains a largely unsolved challenge. Following a similar approach but utilizing a tweezer binding motif, our group reported the preferential oxidation of the deactivated C3/C4 position of aliphatic ammonium substrates.[24,25]

However, the site-selective C–H oxidation of linear alkanes devoid of functional groups has not been achieved. Even in the broader field of C–H functionalization, the site-selective derivatization of unfunctionalized linear alkanes still poses a great challenge.[26] The Hartwig group reported the C1-selective borylation of alkanes.[27] In a further landmark achievement, the Davies group succeeded in the highly C2-selective carbene insertion of aryl diazoacetates into linear alkanes by employing a bulky dirhodium catalyst.[28] The utilization of even bulkier catalysts resulted in the preferential oxidation of the even less reactive terminal C1 position.[29]

Here, we report that the supramolecular catalyst Mn(mcp)-RS_2 enables the preferential oxidation of C(sp^3)–H bonds at the fifth position from the less hindered side on aliphatic substrates devoid of functional handles (Figure 1B).

RESULTS AND DISCUSSION

Control of site selectivity was achieved through the construction of catalysts equipped with a recognition motif able to bind substrates, mainly because of the solvophobic effect and potentially also dispersion interactions, to enable interactions independent of specific functional groups.[30–32] This seems extremely challenging in organic solvents required for state-of-the-art C–H oxidation catalysts, such as **1**–**3**. However, the Diederich group demonstrated that the solvophobic effect in trifluoroethanol (TFE), a solvent of choice for C–H oxidations,[33] is very close to the hydrophobic effect in water.[34] They showed that the empirical solvent polarity parameter E_T correlates very well with the binding strength of apolar guests. Although TFE (normalized E_T^N = 0.898) is already quite close to water (E_T^N = 1.00), 1,1,1,3,3,3-hexafluoro-2-propanol (HFIP), another solvent of choice for C–H oxidations,[33] approximately matches the solvophobic effect of water according to this parameter.[35] Thus, the binding of apolar substrates in suitable binding motifs is facilitated similarly in these fluorinated solvents (solvophobic effect) and water (hydrophobic effect). We demonstrate that this binding can be translated to site-selective C–H oxidation.

The catalyst design consists of a Mn(mcp) (**3**) oxidation core[36,37] to which two resorcin[4]arene (RS) recognition motifs are attached on the pyridine 5 positions. The RS motif was chosen because it is suitably sized to bind methyl groups.[38] Its synthesis started from the literature-known methyl-RS (**5**; Scheme 1),[39] which was subjected to mono-bromination, followed by installation of the methylene bridges at the phenol moieties to deliver bromide **6**. Subsequent *Miyaura* borylation and *Suzuki* cross-coupling with **7** yielded aldehyde **8**. Reduction with sodium borohydride and *Appel* bromination with *N*-bromosuccinimide (NBS) resulted in benzylic bromide **9**. Finally, double alkylation of diamine **10** yielded ligand **11**, which gave the catalyst Mn(mcp)-RS_2 (**4**) after coordination with $Mn(OTf)_2$. Crystals suitable for X-ray diffraction analysis were obtained via vapor diffusion and slow evaporation techniques, revealing the arrangement of the RS binding pockets toward each other in a slightly twisted conformation.

With catalyst **4** in hand, we started the oxidation experiments by utilizing octane as a substrate that, according to molecular modeling (see Figure S45), was of suitable length to bind to both recognition pockets. We explored slightly modified standard oxidation conditions[22] (1.0 mol % catalyst, 22 equiv acetic acid [AcOH], 2.0 equiv H_2O_2 in MeCN or 1.0 equiv H_2O_2 in fluorinated alcohols, ice bath, 1 h). To facilitate analysis, we oxidized the initially formed oxidation products (mainly alcohols) with 2-iodoxybenzoic acid (IBX) to ketones (see Scheme 2 and supplemental information section "general oxidation procedure" for details). Although the ketone products dominated in all cases, two further oxidation products,[40] esters and epoxides, were identified (see Scheme 2 and supplemental information section

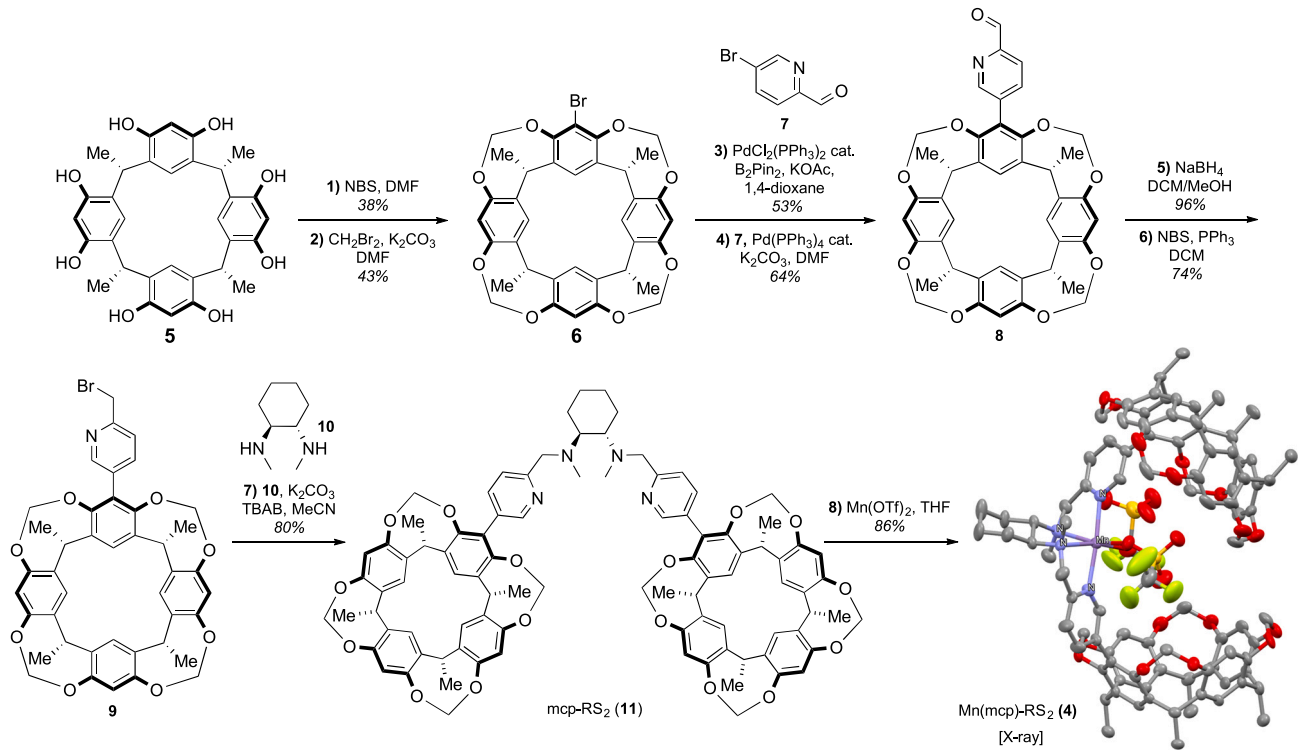

Scheme 1. Synthesis route of catalyst 4

"identification of all oxidation products of octane (S2)" for details; the results of catalyst **4** are highlighted in bold). The bottom left of Scheme 2 describes the C4 selectivity, and the right shows conversion and yield (see Figure S4 for a visual depiction). As expected, in acetonitrile, a solvent of relatively low polarity (E_T^N = 0.460),[35] the C4 selectivity for supramolecular catalyst **4** (31%) was nearly identical to that of control **3**, devoid of recognition motifs (30%; Scheme 2 entry 1, MeCN column). However, when moving to the much more polar fluorinated alcohols, we observed a significant increase in C4 selectivity: 41% in TFE, 46% in HFIP, and 52% in nonafluoro-*tert*-butyl alcohol (NFTBA). Importantly, as expected, the site selectivity for unsubstituted control catalyst **3** was not influenced by solvent polarity. These initial results supported our hypothesis that the solvophobic effect is important for substrate binding in the cavity created by catalyst **4**.

Next, we varied the acid additive, which has been demonstrated to have a pronounced influence on C–H oxidation selectivity.[42,43] Although the acid size did not significantly influence the C4 selectivity in acetonitrile (Scheme 2 entries 1–4, MeCN column), we observed an interesting finding in TFE. The C4 site selectivity increased substantially with acid bulkiness: 41% with AcOH, 62% with propanoic acid (PA), 71% with 2-methylpropanoic acid (2-Me-PA), and 79% ± 1.6% with 2,2-dimethylpropanoic acid (2,2-DiMe-PA). We repeated the experiment five times to judge the reproducibility of these values. Surprisingly, the influence of the acid additive was weaker for HFIP (46% → 67% C4 selectivity) and completely absent in NFTBA. We suspect that the bulky acid helps in creating a more encompassing cavity around the catalytically active center to improve substrate binding and thus selectivity in TFE. Analysis of the amount of ester side products formed seemed to indicate that the more polar solvents (HFIP and especially NFTBA) more effectively compete with the carboxylic acid additive for binding to the active site and thus potentially reduce the selectivity effect of the carboxylic acid (see supplemental information section "investigations on the role of the carboxylic acid additive and fluorinated alcohols" for details).

Next, we assessed whether the observed site selectivity could be rationalized computationally. Thus, we conformationally optimized catalyst **4** (geometry based on the X-ray structure) binding octane by using the global optimizer algorithm (GOAT; ORCA Manual 6.0, xTB-GFN2 method, ALPB [WATER] solvation model). We employed this structure to initialize a Born-Oppenheimer molecular dynamics (MD) simulation according to the xTB-GFN2 method (see supplemental information, computational part).[44–47] The analysis revealed that over the simulation time period of 40 ps, the central C atoms, C4 = C5, (1) were on average closest to the reaction site (see Figure S46) and (2) displayed the absolute shortest (Mn=)O–C distances and thus the most likely ones to be oxidized.

We performed the following control experiments to assess the catalyst design of **4**. First, we explored the separation of the recognition motif (**12**) from oxidation catalyst **3** (Figure 2, gas chromatography [GC] chromatogram B). We observed the same site selectivity as displayed by the unsubstituted catalyst **3** itself (A). Second, the mono-functionalized catalyst Mn(mcp)-RS_1 (**13**, C), carrying only one RS binding motif, exhibited some enhanced C4 selectivity (53%) but failed to reach the

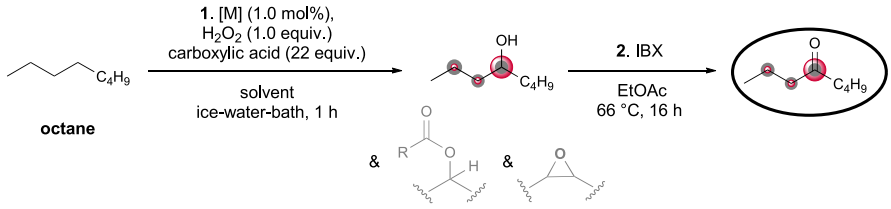

[M]: **Mn(mcp)-RS$_2$ (4)** | Mn(mcp) (**3**)

		C4 Selectivity (%)[a]								Conversion[b] | Yield (%)[c]							
	Entry	MeCN[d]		TFE		HFIP		NFTBA		MeCN		TFE		HFIP		NFTBA	
AcOH	1	**31**	30	**41**	32	**46**	34	**52**	31	**74/42**	73/41	**64/33**	72/34	**67/38**	95/50	**96/68**	81/50
PA	2	**33**	29	**62**	32	**60**	31	**53**	31	**65/34**	58/27	**61/34**	69/32	**61/27**	82/49	**85/61**	88/56
2-Me-PA	3	**32**	29	**71**	32	**61**	29	**54**	32	**48/19**	41/11	**63/29**	53/18	**41/29**	58/29	**82/57**	78/48
2,2-DiMe-PA	4	**36**	28	**79±1.6**	30±0.9	**67**	30	**52**	35	**64/26**	65/27	**80[e]/47[f]**	73[g]/37[h]	**77/50**	78/54	**77/48**	89/53

Scheme 2. Oxidation of octane: General reaction overview and condition optimization

General reaction conditions: 1.0 mol % catalyst, 22 equiv carboxylic acid, 1.0 equiv H_2O_2, ice bath, 1 h; followed by IBX oxidation to convert alcohol products to ketones.

[a]Site selectivity of carbon (Cx) calculated as the GC yield of a particular ketone (adjusted with the calculated response factor[25,41])/total GC yield of all mono-ketones. Oxidation selectivities of catalysts **3** and **4** are displayed as gray and red spheres, respectively.

[b]Conversion calculated on the basis of the remaining substrate.

[c]GC yield equals the sum of all mono-ketones.

[d]2.0 equiv of H_2O_2. Further details regarding the C–H oxidation procedure in MeCN can be found in supplemental information section "general oxidation procedure."

[e]±6.6 (standard deviation).

[f]±5.2.

[g]±4.2.

[h]±4.3.

79% selectivity of the fully functionalized catalyst **4** (D). These control experiments confirmed (1) that a covalent attachment of the recognition motifs is required and (2) that both recognition motifs contribute to the selectivity observed.

Subsequently, we explored the scope of the reaction. We studied a series of linear alkanes and 1-halo alkanes of varying lengths (**S1**–**S15**; Figure 3). For all examples investigated, we observed that the oxidation with supramolecular catalyst **4** preferentially took place at the fifth position in the chain (highlighted by a red solid sphere in Figure 3, counting from the carbon/halogen atom marked with a gray circle; for a more detailed visual depiction of the selectivities, see supplemental information section "substrate scope and detailed oxidation results"). In comparison with reference catalyst **3**, alkanes **S2**, **S7**, and **S12** showed the biggest selectivity increase in percentage points.

Next, we investigated branched alkanes **S16**–**S18**. Again, we observed preferred oxidation at the fifth position from the less hindered side, except that **S18** featured a tertiary C–H bond adjacent to this position (*vide infra*). For **S16**, the tertiary C–H bond at C3 was oxidized preferentially (63%) by **4**, whereas reference catalyst **3** favored C2 (52%) over C3 (23%). This finding shows that catalyst **4** is capable of distinguishing between two adjacent tertiary C–H bonds. The intrinsic reactivity of C–H bonds[48] was overridden in the case of **S17**, where the less reactive secondary C(5)–H bond (46%) was preferred by **4** over the more reactive tertiary C(2)–H bond (21%). In comparison, catalyst **3** favored C2 (45%) over C5 (12%). Substrate **S18** is interesting because it features an electronically deactivated tertiary C(3)–H bond (Figure 3, dashed red circle). This makes the remote tertiary C(7)–H bond the favorable one for electrophilic catalysts,[48] such as **3** (C7: 96%; C3: 4%). Despite having the same core, **4** was capable of overriding its core's intrinsic bias and oxidized the C3 position preferentially (57%). Interestingly, no oxidation of the secondary C(4)–H bond on the fifth position of **S18** was apparent, most likely because of its close proximity to the more reactive tertiary C–H bond on C3.

Finally, we explored a cyclic substrate, *trans-p*-menthane (**S19**). Again, **4** exhibited enhanced selectivity toward C4 (Figure 3, fifth position from the gray circle). The selectivity observed (49%) for the sterically highly congested medial C4 position was impressive given that the regular, non-modified catalyst **3** displayed only 4% selectivity for this site.

In conclusion, we have developed catalyst **4**, which enables substrate binding primarily through the solvophobic effect and possibly dispersion interactions rather than relying on specific interactions of functional groups. This approach is only feasible in fluorinated solvents, such as TFE. This solvent displays a solvophobic effect close to the hydrophobic effect of water but, in contrast to water, is compatible with the oxidation process. Catalyst **4** directed C–H oxidations to the fifth position on the chain of alkane substrates. This is noteworthy because such positions cannot be addressed with state-of-the-art oxidation catalysts. Even in the broader field of C–H functionalization, the functionalization of such a position on linear alkanes is unprecedented. The usage of a bulky carboxylic acid additive improved the selectivity substantially, most likely because of the creation of a more encompassing binding site. As expected, no significant product inhibition was observed. With 1 mol % of the supramolecular

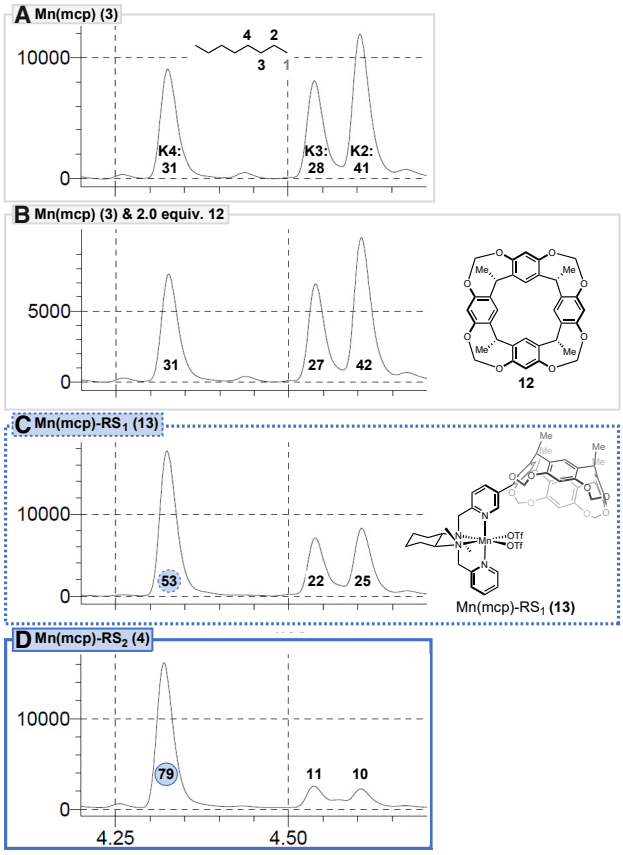

Figure 2. Assessment of four different catalyst designs by GC

Reactions carried out in TFE with 2,2-DiMe-PA according to the general oxidation procedure described in Scheme 2. Conv, conversion; Kx, ketone on carbon x.

(A) **3**.

(B) **3** + RS derivative **12** (2.0 equiv in relation to **3**).

(C) Mono-substituted **13**.

(D) **4**.

catalyst, conversions in the range of 60%–70% were typically observed. The lack of significant product inhibition was most likely due to the higher polarity of the oxidized products than of the substrates, which reduced their solvophobic binding strength. This study opens up new horizons for the site-selective C–H oxidation in hydrocarbon skeletons that lack functional handles, which have traditionally been required for directing C–H oxidation away from the intrinsically most reactive sites.

METHODS

General C–H oxidation procedure in fluorinated alcohols:

(1) According to a modified literature-known procedure,[24] a solution of carboxylic acid additive **A** in fluorinated alcohol **B** (2.0 M, 200 μL, 407 μmol, 22 equiv unless specified otherwise) and substrate **Sx** (18.5 μmol, 1.0 equiv) were added to a 2.0 mL vial charged with catalyst **[M]** (1.0 mol %) and a stirring bar. The mixture was cooled in an ice-water bath. Next, a solution of H_2O_2 (50 wt % diluted in solvent **B**, 0.9 M, 20.6 μL, 18.5 μmol, 1.0 equiv unless otherwise specified) was slowly added over 15 min via a syringe pump. The reaction mixture was stirred for a further 45 min. Subsequently, H_2O (1.5 mL) and a solution of biphenyl in ethyl acetate (92.5 mM, 40 μL, 3.70 μmol, 0.20 equiv) were added. The mixture was extracted with ethyl acetate (2 × 1.5 mL), and the combined organic layers were washed with a saturated solution of $NaHCO_3$ (2.0 mL), followed by H_2O (2.0 mL), dried over Na_2SO_4, and filtered through a silica plug. The mixture was analyzed via GC and GC-mass spectrometry (GC-MS).

(2) To facilitate analysis, we performed subsequent oxidation of the alcohol products to ketones with IBX: 0.5 mL of the crude mixture (ca. 3.0 mL) was added to a 2 mL vial charged with IBX (3.50 mg, 12.5 μmol) and a stirring bar. The vial was sealed with a Teflon tap, and the mixture was heated to 66°C (temperature of the aluminum heating block) for 16 h. After cooling down to room temperature, the mixture was filtered through a silica plug, and the vial was rinsed with ethyl acetate (2 × 1.0 mL). GC and GC-MS analyses were conducted.

Further details regarding the C–H oxidation procedures can be found in the supplemental methods (supplemental information section "oxidation studies").

RESOURCE AVAILABILITY

Lead contact

Requests for further information and resources should be directed to and will be fulfilled by the lead contact, Konrad Tiefenbacher (konrad.tiefenbacher@unibas.ch).

Materials availability

Compounds synthesized in this work will be made available on request, but we might require a payment and/or a completed materials transfer agreement if there is potential for commercial application.

Methods, intermediate and product characterizations, detailed results on C–H oxidation studies, etc., are described in the supplemental information. Crystallographic data are available from the Cambridge Crystallographic Data Center (CCDC) under deposition number CCDC: 2382829.

Data and code availability

All data supporting the conclusions of this work are presented in the main text or the supplemental information. Raw data, spectra, and GC chromatograms can be found at Zenodo: 13828916.

ACKNOWLEDGMENTS

We thank Dr. Michael Pfeffer for the high-resolution mass spectrometry analysis, the National Centre of Competence in Research (NCCR) Molecular Systems Engineering for financial support, and the computing center of the University of Cologne (RRZK) for providing CPU time on the DFG-funded supercomputer CHEOPS.

AUTHOR CONTRIBUTIONS

K.T. conceived and supervised the project. Y.L. planned, performed, and analyzed the experimental work. M.K. performed the initial experiments. A.P. solved and refined the X-ray crystal structure. B.G. performed and analyzed

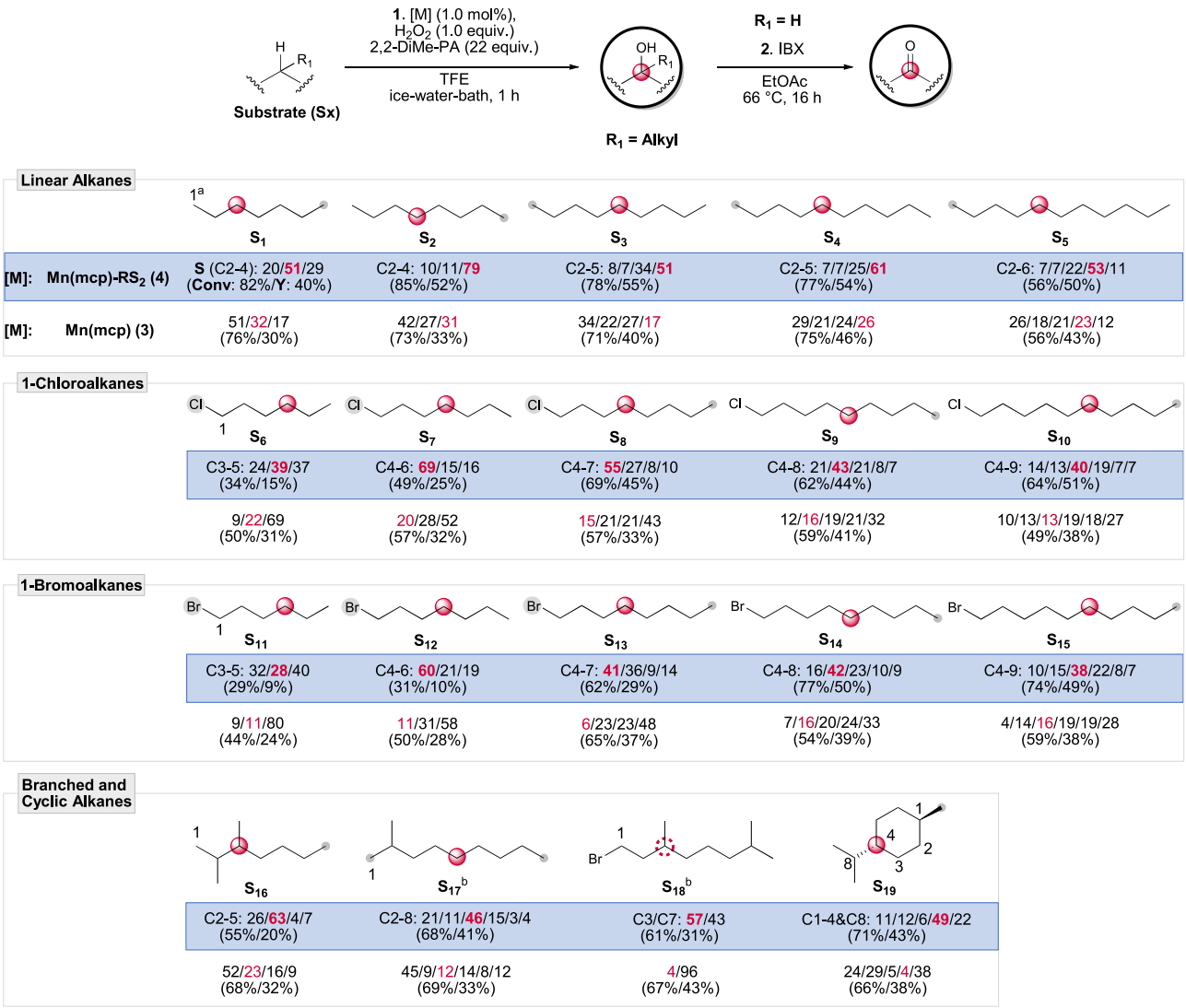

Figure 3. Substrates investigated in this work

S, site selectivity (on carbon Cx, given in %); conv, conversion; Y, yield. The fifth position is highlighted by the red solid sphere counting from the end(s) marked with a gray circle.

[a]C1 according to the International Union of Pure and Applied Chemistry (IUPAC).

[b]5.0 equiv of acid used.

the calculations. K.T. and Y.L. compiled the first draft of the manuscript. All authors contributed to the final version of the manuscript.

DECLARATION OF INTERESTS

The authors declare no competing interests.

SUPPLEMENTAL INFORMATION

Supplemental information can be found online at https://doi.org/10.1016/j.chempr.2025.102442.

Received: September 26, 2024
Revised: December 2, 2024
Accepted: January 16, 2025
Published: February 25, 2025

REFERENCES

1. (2024). Handbook of chemistry and physics, J. Rumle, ed. (Routledge & CRC Press). https://www.routledge.com/CRC-Handbook-of-Chemistry-and-Physics/Rumble/p/book/9781032655628.

2. Bordwell, F.G. (1988). Equilibrium acidities in dimethyl sulfoxide solution. Acc. Chem. Res. *21*, 456–463. https://doi.org/10.1021/ar00156a004.

3. Gormisky, P.E., and White, M.C. (2013). Catalyst-controlled aliphatic C–H oxidations with a predictive model for site-selectivity. J. Am. Chem. Soc. *135*, 14052–14055. https://doi.org/10.1021/ja407388y.

4. Font, D., Canta, M., Milan, M., Cussó, O., Ribas, X., Klein Gebbink, R.J.M., and Costas, M. (2016). Readily accessible bulky iron catalysts exhibiting site selectivity in the oxidation of steroidal substrates. Angew. Chem. Int. Ed. *55*, 5776–5779. https://doi.org/10.1002/anie.201600785.

5. White, M.C., and Zhao, J. (2018). Aliphatic C–H oxidations for late-stage functionalization. J. Am. Chem. Soc. *140*, 13988–14009. https://doi.org/10.1021/jacs.8b05195.

6. Newhouse, T., and Baran, P.S. (2011). If C–H bonds could talk: selective C–H bond oxidation. Angew. Chem. Int. Ed. *50*, 3362–3374. https://doi.org/10.1002/anie.201006368.

7. Curci, R., D'Accolti, L., and Fusco, C. (2006). A novel approach to the efficient oxygenation of hydrocarbons under mild conditions. Superior oxo transfer selectivity using dioxiranes. Acc. Chem. Res. *39*, 1–9. https://doi.org/10.1021/ar050163y.

8. D'Accolti, L., Annese, C., and Fusco, C. (2019). Continued progress towards efficient functionalization of natural and non-natural targets under mild conditions: oxygenation by C−H Bond activation with dioxirane. Chem. Eur. J. *25*, 12003–12017. https://doi.org/10.1002/chem.201901687.

9. Breslow, R., Dale, J.A., Kalicky, P., Liu, S.Y., and Washburn, W.N. (1972). Introduction of a 9(11) double bond into steroids by selective free-radical halogenation. J. Am. Chem. Soc. *94*, 3276–3278. https://doi.org/10.1021/ja00764a085.

10. Breslow, R., Corcoran, R.J., Snider, B.B., Doll, R.J., Khanna, P.L., and Kaleya, R. (1977). Selective halogenation of steroids using attached aryl iodide templates. J. Am. Chem. Soc. *99*, 905–915. https://doi.org/10.1021/ja00445a038.

11. Chen, K., Richter, J.M., and Baran, P.S. (2008). 1,3-Diol synthesis via controlled, radical-mediated C–H functionalization. J. Am. Chem. Soc. *130*, 7247–7249. https://doi.org/10.1021/ja802491q.

12. Simmons, E.M., and Hartwig, J.F. (2012). Catalytic functionalization of unactivated primary C–H bonds directed by an alcohol. Nature *483*, 70–73. https://doi.org/10.1038/nature10785.

13. Bigi, M.A., Reed, S.A., and White, M.C. (2012). Directed metal (oxo) aliphatic C–H hydroxylations: overriding substrate bias. J. Am. Chem. Soc. *134*, 9721–9726. https://doi.org/10.1021/ja301685r.

14. Frost, J.R., Huber, S.M., Breitenlechner, S., Bannwarth, C., and Bach, T. (2015). Enantiotopos-selective C–H oxygenation catalyzed by a supramolecular ruthenium complex. Angew. Chem. Int. Ed. *54*, 691–695. https://doi.org/10.1002/anie.201409224.

15. Burg, F., Gicquel, M., Breitenlechner, S., Pöthig, A., and Bach, T. (2018). Site- and enantioselective C−H oxygenation catalyzed by a chiral manganese porphyrin complex with a remote binding site. Angew. Chem. Int. Ed. *57*, 2953–2957. https://doi.org/10.1002/anie.201712340.

16. Burg, F., Breitenlechner, S., Jandl, C., and Bach, T. (2020). Enantioselective oxygenation of exocyclic methylene groups by a manganese porphyrin catalyst with a chiral recognition site. Chem. Sci. *11*, 2121–2129. https://doi.org/10.1039/C9SC06089H.

17. Breslow, R., Gabriele, B., and Yang, J. (1998). Geometrically directed selective steroid hydroxylation with high turnover by a fluorinated artificial cytochrome P-450. Tetrahedron Lett. *39*, 2887–2890. https://doi.org/10.1016/S0040-4039(98)00425-0.

18. Breslow, R., and Dong, S.D. (1998). Biomimetic reactions catalyzed by cyclodextrins and their derivatives. Chem. Rev. *98*, 1997–2012. https://doi.org/10.1021/cr970011j.

19. Das, S., Incarvito, C.D., Crabtree, R.H., and Brudvig, G.W. (2006). Molecular recognition in the selective oxygenation of saturated C–H bonds by a dimanganese catalyst. Science *312*, 1941–1943. https://doi.org/10.1126/science.1127899.

20. Das, S., Brudvig, G.W., and Crabtree, R.H. (2008). High turnover remote catalytic oxygenation of alkyl groups: how steric exclusion of unbound substrate contributes to high molecular recognition selectivity. J. Am. Chem. Soc. *130*, 1628–1637. https://doi.org/10.1021/ja076039m.

21. Olivo, G., Capocasa, G., Ticconi, B., Lanzalunga, O., Di Stefano, S., and Costas, M. (2020). Predictable selectivity in remote C–H oxidation of steroids: analysis of substrate binding mode. Angew. Chem. Int. Ed. *59*, 12703–12708. https://doi.org/10.1002/anie.202003078.

22. Olivo, G., Farinelli, G., Barbieri, A., Lanzalunga, O., Di Stefano, S., and Costas, M. (2017). Supramolecular recognition allows remote, site-selective C–H oxidation of methylenic sites in linear amines. Angew. Chem. Int. Ed. *56*, 16347–16351. https://doi.org/10.1002/anie.201709280.

23. Olivo, G., Cussó, O., Borrell, M., and Costas, M. (2017). Oxidation of alkane and alkene moieties with biologically inspired nonheme iron catalysts and hydrogen peroxide: from free radicals to stereoselective transformations. J. Biol. Inorg. Chem. *22*, 425–452. https://doi.org/10.1007/s00775-016-1434-z.

24. Knezevic, M., and Tiefenbacher, K. (2023). Tweezer-based C–H oxidation catalysts overriding the intrinsic reactivity of aliphatic ammonium substrates. Chem. Eur. J. *29*, e202203480. https://doi.org/10.1002/chem.202203480.

25. Knezevic, M., Heilmann, M., Piccini, G.M., and Tiefenbacher, K. (2020). Overriding intrinsic reactivity in aliphatic C–H oxidation: preferential C3/C4 oxidation of aliphatic ammonium substrates. Angew. Chem. Int. Ed. *59*, 12387–12391. https://doi.org/10.1002/anie.202004242.

26. Tang, X., Jia, X., and Huang, Z. (2018). Challenges and opportunities for alkane functionalisation using molecular catalysts. Chem. Sci. *9*, 288–299. https://doi.org/10.1039/C7SC03610H.

27. Hartwig, J.F. (2012). Borylation and silylation of C–H bonds: a platform for diverse C–H bond functionalizations. Acc. Chem. Res. *45*, 864–873. https://doi.org/10.1021/ar200206a.

28. Liao, K., Negretti, S., Musaev, D.G., Bacsa, J., and Davies, H.M.L. (2016). Site-selective and stereoselective functionalization of unactivated C–H bonds. Nature *533*, 230–234. https://doi.org/10.1038/nature17651.

29. Liao, K., Yang, Y.-F., Li, Y., Sanders, J.N., Houk, K.N., Musaev, D.G., and Davies, H.M.L. (2018). Design of catalysts for site-selective and enantioselective functionalization of non-activated primary C–H bonds. Nat. Chem. *10*, 1048–1055. https://doi.org/10.1038/s41557-018-0087-7.

30. Schneider, H.-J. (1991). Mechanisms of molecular recognition: investigations of organic host–guest complexes. Angew. Chem. Int. Ed. *30*, 1417–1436. https://doi.org/10.1002/anie.199114171.

31. Murray, J., Kim, K., Ogoshi, T., Yao, W., and Gibb, B.C. (2017). The aqueous supramolecular chemistry of cucurbit[n]urils, pillar[n]arenes and deep-cavity cavitands. Chem. Soc. Rev. *46*, 2479–2496. https://doi.org/10.1039/C7CS00095B.

32. Yu, Y., Yang, J.-M., and Rebek, J. (2020). Molecules in confined spaces: reactivities and possibilities in cavitands. Chem *6*, 1265–1274. https://doi.org/10.1016/j.chempr.2020.04.014.

33. Dantignana, V., Milan, M., Cussó, O., Company, A., Bietti, M., and Costas, M. (2017). Chemoselective aliphatic C–H bond oxidation enabled by polarity reversal. ACS Cent. Sci. *3*, 1350–1358. https://doi.org/10.1021/acscentsci.7b00532.

34. Smithrud, D.B., and Diederich, F. (1990). Strength of molecular complexation of apolar solutes in water and in organic solvents is predictable by linear free energy relationships: a general model for solvation effects on apolar binding. J. Am. Chem. Soc. *112*, 339–343. https://doi.org/10.1021/ja00157a052.

35. Reichardt, C. (1994). Solvatochromic dyes as solvent polarity indicators. Chem. Rev. *94*, 2319–2358. https://doi.org/10.1021/cr00032a005.

36. Murphy, A., Dubois, G., and Stack, T.D.P. (2003). Efficient epoxidation of electron-deficient olefins with a cationic manganese complex. J. Am. Chem. Soc. *125*, 5250–5251. https://doi.org/10.1021/ja029962r.

37. Ottenbacher, R.V., Bryliakov, K.P., and Talsi, E.P. (2010). Nonheme manganese-catalyzed asymmetric oxidation. A Lewis acid activation versus oxygen rebound mechanism: evidence for the "third oxidant". Inorg. Chem. *49*, 8620–8628. https://doi.org/10.1021/ic101297x.

38. Cram, D.J., Karbach, S., Kim, H.E., Knobler, C.B., Maverick, E.F., Ericson, J.L., and Helgeson, R.C. (1988). Host-guest complexation. 46. Cavitands as open molecular vessels form solvates. J. Am. Chem. Soc. *110*, 2229–2237. https://doi.org/10.1021/ja00215a037.

39. Niederl, J.B., and Vogel, H.J. (1940). Aldehyde-resorcinol condensations. J. Am. Chem. Soc. *62*, 2512–2514. https://doi.org/10.1021/ja01866a067.

40. Costas, M. (2021). Site and enantioselective aliphatic C–H oxidation with bioinspired chiral complexes. Chem. Rec. *21*, 4000–4014. https://doi.org/10.1002/tcr.202100227.

41. Scanlon, J.T., and Willis, D.E. (1985). Calculation of flame ionization detector relative response factors using the effective carbon number concept. J. Chromatogr. Sci. *23*, 333–340. https://doi.org/10.1093/chromsci/23.8.333.

42. Lyakin, O.Y., Ottenbacher, R.V., Bryliakov, K.P., and Talsi, E.P. (2012). Asymmetric epoxidations with H_2O_2 on Fe and Mn aminopyridine catalysts: probing the nature of active species by combined electron paramagnetic resonance and enantioselectivity study. ACS Catal. *2*, 1196–1202. https://doi.org/10.1021/cs300205n.

43. Vicens, L., Olivo, G., and Costas, M. (2020). Rational design of bioinspired catalysts for selective oxidations. ACS Catal. *10*, 8611–8631. https://doi.org/10.1021/acscatal.0c02073.

44. Bannwarth, C., Caldeweyher, E., Ehlert, S., Hansen, A., Pracht, P., Seibert, J., Spicher, S., and Grimme, S. (2021). Extended tight-binding quantum chemistry methods. WIREs Comput. Mol. Sci. *11*, e1493. https://doi.org/10.1002/wcms.1493.

45. Bannwarth, C., Ehlert, S., and Grimme, S. (2019). GFN2-xTB—an accurate and broadly parametrized self-consistent tight-binding quantum chemical method with multipole electrostatics and density-dependent dispersion contributions. J. Chem. Theor. Comput. *15*, 1652–1671. https://doi.org/10.1021/acs.jctc.8b01176.

46. Ehlert, S., Stahn, M., Spicher, S., and Grimme, S. (2021). Robust and efficient implicit solvation model for fast semiempirical methods. J. Chem. Theor. Comput. *17*, 4250–4261. https://doi.org/10.1021/acs.jctc.1c00471.

47. Neese, F. (2022). Software update: the ORCA program system—version 5.0. WIREs Comput. Mol. Sci. *12*, e1606. https://doi.org/10.1002/wcms.1606.

48. Chen, M.S., and White, M.C. (2007). A predictably selective aliphatic C–H oxidation reaction for complex molecule synthesis. Science *318*, 783–787. https://doi.org/10.1126/science.1148597.